Gene variant profiles and tumor metabolic activity as measured by *FOXM1* expression and glucose uptake in lung adenocarcinoma

Ashley Goodman[1], Waqas Mahmud[2], Lela Buckingham[1,2]

[1]Rush University College of Health Sciences, Chicago, IL;
[2]Department of Pathology, Rush University Medical Center, Chicago, IL, USA

Background: Cancer cells displaying aberrant metabolism switch energy production from oxidative phosphorylation to glycolysis. Measure of glucose standardized uptake value (SUV) by positron emission tomography (PET), used for staging of adenocarcinoma in high-risk patients, can reflect cellular use of the glycolysis pathway. The transcription factor, FoxM1 plays a role in regulation of glycolytic genes. Cancer cell transformation is driven by mutations in tumor suppressor genes such as *TP53* and *STK11* and oncogenes such as *KRAS* and *EGFR*. In this study, SUV and *FOXM1* gene expression were compared in the background of selected cancer gene mutations. **Methods:** Archival tumor tissue from cases of lung adenocarcinoma were analyzed. SUV was collected from patient records. *FOXM1* gene expression was assessed by quantitative reverse transcriptase polymerase chain reaction (qRT-PCR). Gene mutations were detected by allele-specific PCR and gene sequencing. **Results:** SUV and *FOXM1* gene expression patterns differed in the presence of single and co-existing gene mutations. Gene mutations affected SUV and *FOXM1* differently. *EGFR* mutations were found in tumors with lower *FOXM1* expression but did not affect SUV. Tumors with *TP53* mutations had increased SUV (p = .029). *FOXM1* expression was significantly higher in tumors with *STK11* mutations alone (p < .001) and in combination with *KRAS* or *TP53* mutations (p < .001 and p = .002, respectively). **Conclusions:** Cancer gene mutations may affect tumor metabolic activity. These observations support consideration of tumor cell metabolic state in the presence of gene mutations for optimal prognosis and treatment strategy.

Key Words: Lung neoplasms; Forkhead Box protein M1; KRAS protein, human; Treatment outcome

Lung cancer is the leading cause of cancer death in the United States, with the majority of cases falling into the adenocarcinoma (non-small cell lung cancer [NSCLC]) subgroup. There are a large number of somatic mutations that can lead to biological differences among histologically identical tumors in NSCLC patients. This variability partially accounts for the heterogeneity in disease progression and patient outcome seen among the different cases of NSCLC.

Population studies and clinical trials have led to identification of frequently mutated genes and gene products that serve as therapeutic targets [1,2]. Tumor protein P53, *TP53* is the most frequently mutated gene in cancer, encoding a transcription factor that regulates cell cycle arrest and apoptosis. The Kirsten Rat Sarcoma Viral proto-oncogene, *KRAS*, also frequently mutated in cancer cells, is a membrane-associated protein with intrinsic GTPase activity involved in the regulation of cell proliferation. The epidermal growth factor receptor gene, epidermal growth factor receptor (*EGFR*), encodes a tyrosine kinase membrane receptor identified as a therapeutic target in clinical trials investigating tyrosine kinase inhibitors for treatment of lung cancer. *STK11* encodes a tumor suppressor serine/threonine-protein kinase that controls the activity of AMP-activated protein kinases (AMPK), affecting cell metabolism, cell polarity, apoptosis, and DNA damage response. Current clinical testing includes investigation of these genes along with many others for characterization of tumor mutational status as well as therapeutic strategy. Depending on the testing approach, somatic mutations in one or more cancer genes are frequently detected.

Tumor biochemistry has been proposed as one source of tumor heterogeneity [3]. Aberrant energy metabolism has been well documented, with observations that cancer cells can switch their source of energy production from oxidative phosphorylation to

glycolysis [4,5]. Glucose metabolism in malignant and benign cells is measured using cellular uptake of 18-fluorodeoxyglucose (FDG). FDG is glucose combined with a radionuclide. Malignant cells, growing and metabolizing glucose faster than benign cells, use more of the tracer. Measure of FDG uptake in tumors is expressed in a semiquantitative measure, the standardized uptake value (SUV) which is the ratio of tissue radioactivity concentration (C/T) imaged by positron emission tomography (PET) at a point in time to the injected dose of radioactivity per kilogram of the patient's body weight: (C/T)/(injection dose [MBq]/patient's weight [kg]).

SUV has been proposed as a factor in determining adjuvant chemotherapy for stage 1A NSCLC [6]. A combination of cytology, computed tomography and PET measurement of SUV has been reported to detect 90% of malignancy in lung pleural effusions [7].

Along with massive glucose utilization, there is also a significant increase in lactate production in tumor cells [8]. The conversion into lactate is performed by the enzyme lactate dehydrogenase (LDHA), which has been shown to have increased activity in breast, gynecological, colorectal and lung cancer. LDHA is partially regulated by the Forkhead Box M1 (*FOX M1*) transcription factor. FoxM1 protein bound to the LDHA promoter increases its expression at the mRNA and protein level. In vivo studies showed silencing FoxM1 expression caused a decrease in LDHA expression with a corresponding decrease in lactate production and glucose utilization [9]. Thus, FoxM1 plays a role in cancer cell metabolism, at least through the transcriptional regulation of LDHA. The study also showed that elevated FoxM1 expression correlated with increased cell growth and metastasis. Increased cell proliferation associated with higher *FOXM1* expression can lead to poorer prognosis [10].

FOXM1 expression is genetically and epigenetically controlled. *FOXM1* transcription is one of several targets of the microRNA, miR-149 [11]. An inverse relationship between miR-149 and *FOXM1* has been reported in colon cancer [12]. FoxM1 protein function is regulated through cell signaling. For FoxM1 protein to become active, it must be phosphorylated at particular sites, a modification mainly achieved through the Ras-Raf-Mek signaling cascade [13]. Thus, FoxM1 could be a downstream target of the Ras oncogenic signaling cascade and Ras is required for FoxM1 activation through phosphorylation. Conversely, FoxM1 may also be necessary for Kras-mediated changes in expression of several different target genes involved in homeostasis, metabolism and tumor growth [14]. Using a mouse model of NSCLC, it was found that the presence of an activating mutation in *KRAS*,

$Kras^{G12D}$, with simultaneous deletion of *FOXM1*, was sufficient to initiate uncontrolled respiratory epithelial cell proliferation or hyperplasia, but this single stimulus was not enough to progress the hyperplasia into full lung cancer [15]. Therefore, FoxM1 is not necessary for increased cell proliferation of respiratory epithelial cells, but is required for true tumorigenesis. This dependent relationship between Kras and FoxM1 suggests a role for the two genes in increased tumorigenicity and thus affect the overall clinical outcome.

This study assessed the relationship between tumor mutational status and tumor glucose metabolism as measured by standardized glucose uptake volume (SUV) and *FOXM1* gene expression. The results support the consideration of tumor metabolic state in the interpretation of mutation status in NSCLC.

MATERIALS AND METHODS

Patient samples

Analysis of archival tissue in the current study was approved by the Rush University Institutional Review Board (IRB#1212 1202). Participants were deidentified before group statistical analyses. Patient samples consisted of formalin-fixed paraffin-embedded tissue from 301 patients with adenocarcinoma NSCLC (stage I–III) treated at Rush Medical Center through surgical resection and no adjuvant therapy. The study includes cases of adenocarcinoma only.

PET analysis

Tumor metabolic activity was assessed by measure of glucose metabolism (rate of consumption of glucose) through accumulation of FDG. Benign and malignant tumors differ in FDG SUV measured by PET. PET data, measured from tumor tissue prior to surgery, was collected from electronic medical records. When the tumors are imaged by PET, a minimum (PET Min) and maximum (PET Max) density of FDG is reported for the tissue regions scanned. A high (PET Max) and low (PET Min) density was recorded for 301 patients (Table 1). PET Max is considered the maximum SUV of the tissue.

Gene expression analysis

The amount of mRNA expression of the *FOXM1* gene was measured in tumor and non-malignant lung tissue in all patient samples with available corresponding sample material. Hematoxylin and eosin-stained 4-micron sections were reviewed by a pathologist to distinguish tumor and non-malignant tissue for each sample. Tissue was then macro-dissected from the adjacent

Table 1. Patient demographics tumor genetic profile (n=301)

		SUV		Gene expression[a]	Mutation status, n (%)[b]			
	No.	PET Min	PET Max	FOXM1/miR-149	EGFR	KRAS	STK11	TP53
Total	301	2.47±1.44	8.85±6.69	3.11±4.69/3.92±9.84	32/267 (12)	105/296 (35)	17/173 (10)	73/173 (42)
Sex								
Female	168	2.33	8.79	1.83/5.94	22/152	61/167	7/99	40/99
Male	133	2.65	8.93	4.38/1.39	9/115	42/123	10/73	32/73
p-value		.077	.867	.055	.661	.675	.150	.652
Age (yr)								
<60	70	2.48	8.99	0.76/3.30	9/53	17/69	4/42	20/42
>60	231	2.47	8.82	17.3/2.25	22/212	85/227	13/126	51/128
p-value		.973	.857	.002	.181	.050	.882	.462
Smoking[c]								
Ever	56	2.16	10.3	-/0.00	2/40	24/53	8/53	34/53
Non-smoker	17	1.87	8.62	-/2.84	3/10	3/17	0/17	5/17
p-value		.527	.529	-	.018	.042	.089	.012

SUV, standardized uptake value; PET, positron emission tomography.
[a]Expression normalized to B2M; left-tailed probability of the chi-square distribution; [b]Mutated/total resulted; left-tailed probability of the chi-square distribution; [c]Smoking status was not available for all cases.

unstained slide and the RNA extracted using the RecoverAll Total Nucleic Acid Isolation Kit (Ambion/Life Technologies, Austin, TX, USA) according to manufacturer's directions.

Ten microliters of the extracted RNA were converted to cDNA in a reaction mix (Thermo Fisher Scientific, Waltham, MA, USA) containing 5 μL 5× reaction buffer, 2 μL 0.1M DTT, 1 μL each of RNasin (40 units/μL) dNTPs (2.5 mM each) and Moloney virus reverse transcriptase (200 units/μL), yielding 20 μL total volume. Gene expression levels were then measured from the cDNA using TaqMan qRT-PCR. Two microliters of cDNA were mixed with 1.25 μL primer/probe mix (Integrated DNA Technologies, Coralville, IW, USA), 12.5 μL Universal Master Mix with passive reference dye (Roche Diagnostics/Sigma, Mannheim, Germany) brought to a final volume of 25 μL with nuclease-free water. The primers used for FOXM1 were F: 5'-GATGGC-GAATTGTATCATGGC, R: 5'-GGAGGAAAAGGAGA-ATTGTCAC and probe: 5'-/56-FAM/CAGCGACAG/ZEN/GTTAAGGTTGAGGAGC/3lABkFQ and those used for miR-149 were F: 5'-CGTTGTTCCAGCTGCCCCAGC, R: 5'-GCTCCCAGGCCGGCGCC and probe: 5'-/56-FAM/AGACA/ZEN/CGGAGCCAGA/3lABkFQ. In addition to well to well correction through the passive reference dye, the mRNA levels of the housekeeping gene, beta-2 microglobulin (B2M; Integrated DNA Technologies), were concurrently measured in duplicate samples as a cDNA input normalization control. For statistical analysis, target gene expression was normalized to the amount of B2M expression, to compensate for variability in the amount of tissue used and the input cDNA of each sample.

Mutation status

KRAS mutation status was measured from column purified, diluted tissue DNA using the Therascreen PCR method (Qiagen, Hilden, Germany) according to manufacturer's directions. Further variant information was collected from a clinical next-generation sequencing panel of 500 genes (Foundation Medicine, Cambridge, MA, USA).

Statistics

Statistical analysis was performed using SPSS software ver. 18.0 (SPSS Inc., Chicago, IL, USA). Association between gene expression and tumor mutation status was analyzed using the independent T-test. Nonparametric data were analyzed by the Mann-Whitney U test. Association of dichotomized gene expression and mutation status with patient outcome (time to recurrence [TTR] and overall survival [OS]) was analyzed for significance using Kaplan-Meier survival curves.

Ethics statement

All procedures performed in the current study were approved by the Rush University Institutional Review Board (IRB#1212 1202, approved date 3/22/18) with a waiver of individual consent in accordance with the Common Rule (45CFR46, December 13, 2001) and any other governing regulations or subparts. The Institutional Federalwide Assurance Number is FWA000 00482 in accordance with the 1964 Helsinki declaration and its later amendments.

RESULTS

Patient demographics and PET activity

FDG uptake reflects active glucose metabolism in tumor cells but is not constant across tumor tissue. PET Min and PET Max define the low and high metabolic activity of cells, respectively, for each tumor. PET Max is a measure of the maximum metabolic activity of the tumor. Nucleic acid was successfully extracted from 301 archival tissue samples for analysis (Table 1). Tested patients had an average age of 66.8 years (range, 40 to 92 years), were 44% male, and 77% ever smokers. Tumor PET activity was similar in demographic groups, except for marginally increased PET Min in tumors from male patients. It is noted that younger and older patients are not evenly represented in the patient group: 77% of patients were older than 60 years. PET Max (maximum SUV) was not significantly different by sex.

Mutation status

Mutation status was assessed by allele-specific PCR, Sanger sequencing and/or next-generation sequencing of tumor tissue (Table 1). *EGFR* mutations were present in 12% of cases. Fourteen percent of female patient tumors had *EGFR* mutations compared to 8% of male patient tumors. Exon 19 deletions (n = 15) and L858R point mutations (n = 5) accounted for the majority of *EGFR* variants in this patient group.

KRAS mutations present in 35% of cases were equally represented by sex (36% vs. 34% in females and males, respectively). Of the 105 *KRAS* mutations, the most common variants were G12C (n = 42) and G12D (n = 22), and G12V (n = 20). *TP53* is the most mutated gene in cancer and was the most frequently mutated gene in this patient group. *TP53* mutation frequency was 42%, about equally represented in male (40%) and female (44%) patients. The spectrum of *TP53* mutations fell mostly

within the DNA binding domain of the protein.

Chi-square analysis revealed significantly increased mutation frequency in smokers compared to non-smokers for *KRAS* (p = .042) and *TP53* (p = .012). The reverse was true for *EGFR*, where 30% of non-smokers had *EGFR* mutated tumors, compared to 5% of those in smokers (p = .018). Older patients had increased *KRAS* mutations (p = .042).
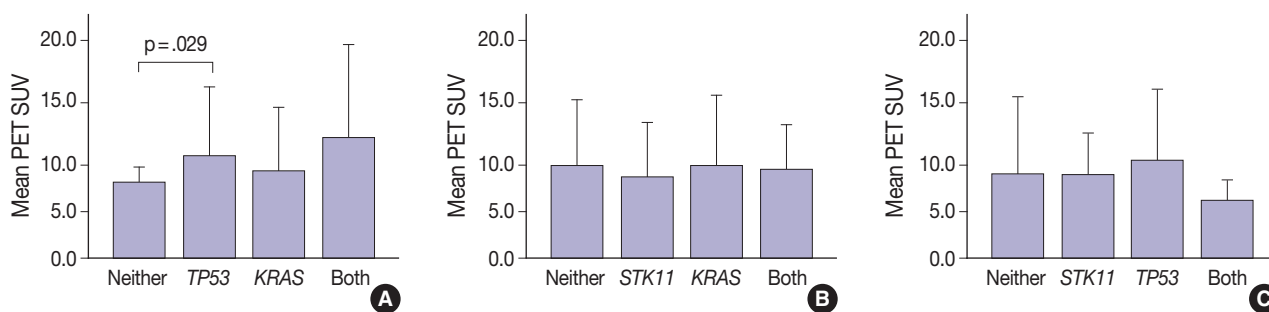
Metabolic activity as measured by SUV vs. gene mutation status

Maximal SUV was assessed in tumor tissue. There was no significant difference in SUV with *KRAS* nor *EGFR* mutation compared to no mutation (p = .443) nor with any *TP53* nor *STK11* mutations (p = .114 and p = .191, respectively) (Fig. 1). Mutation status for all genes were grouped as "mutated" vs. "not mutated." Similar grouping was done for *STK11* due to the low number of *STK11* mutant cases.

Median SUV did not differ significantly among the most fre-
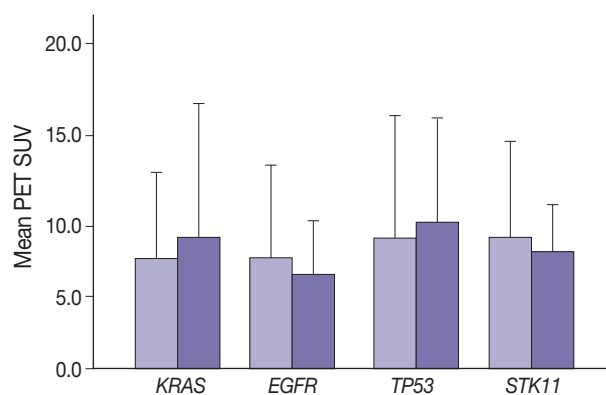
Fig. 1. Maximum positron emission tomography (PET) standardized uptake value (SUV) in the presence of mutations (darker bars) in *KRAS* (p = .089) (A), *EGFR* (p = .443) (B), *TP53* (p = .114) (C), and *STK11* (p = .191) (D).

Fig. 2. Metabolic activity as measured by positron emission tomography (PET) standardized uptake value (SUV) in the presence of multiple mutations. Tumors with *TP53* and *KRAS* mutations together had higher SUV (p = .029 vs. no mutations) (A). No significant differences in SUV were observed in tumors with *KRAS* with and without *STK11* mutations (B). Tumors with *STK11* and *TP53* mutations had marginally decreased SUV (p = .141 vs. TP53 only) (C).

quent *KRAS* mutations. For 170 wild-type, 31 G12C, 22 G12D, 19 G12V, and 14 other *KRAS* mutations, median SUV ranged from 6.4 (G12D) to 8.4 (G12V). Median SUV in the absence of any KRAS was 7.4.

Thirty-one tumors displayed mutations in more than one oncogene. Tumor metabolic activity measured by PET was compared in the presence of these mutation profiles (n = 168) (Fig. 2). Tumors with co-existing *KRAS* and *TP53* mutations showed higher metabolic activity (p = .029) (Fig. 2A). The presence of single *KRAS* and *STK11* mutations vs. combinations showed no significant relationship to metabolic activity (Fig. 2B). FDG uptake was lower in the presence of *STK11* mutations when *TP53* mutations were present, but not significantly so (Fig. 2C).

Metabolic activity as measured by *FOXM1* gene expression

The role of *FOXM1* in glycolysis along with its tumor suppressor potential led to assessing its association with tumor metabolic activity. *FOXM1* is epigenetically regulated, in part, by miRNA, specifically miR-149, the expression of which was also measured. The amount of *FOXM1* and miR-149 expression in the tumor samples was assessed by quantitative reverse transcriptase PCR normalized to B2M expression. There was significantly higher *FOXM1* expression in tumor tissue from older patients accompanied by half the miR-149 expression (chi-square p = .002) (Table 1).

Compared to non-malignant tissue, *FOXM1* transcription is increased in tumor cells. To confirm this, mRNA was isolated from adjacent non-malignant lung tissue to estimate endogenous *FOXM1* expression before the oncogenic transformation. Only two of the 34 normal tissue samples tested were positive for *FOXM1* expression (5.9%) indicating that expression differences were not likely due to differences in endogenous levels of gene expression between patients, but *FOXM1* was specifically induced in and unique to the tumor cells (*FOXM1*/B2M% 8.65 tumor vs. 1.67 normal; p < .001).

Because miR-149 negatively regulates *FOXM1*, an inverse expression pattern between the two genes might be expected. *FOXM1* expression was inversely proportional to miR-149 expression, 13.6 *FOXM1*/B2M% with no detectable miR-149 expression versus 4.6 with miR-149 expression. If both gene activities were dichotomized (expressed/not expressed), cross-tabulation showed more cases of *FOXM1* expressed when miR-149 was not detected, consistent with an inverse relationship which was also observed in dichotomized data for both genes (expressed/not expressed).

FOXM1 expression in the tumor samples was compared to

metabolic activity as measured by SUV from FDG-PET imaging. SUV (minimal and maximal) were higher with any *FOXM1* expression compared to no detectable *FOXM1* (avg. maximum SUV, 8.90 vs. 6.8 [p = .425]; avg. minimal SUV, 2.62 vs. 2.02 [p = .069] with and without *FOXM1*, respectively).

## *FOXM1* gene expression and mutation status

Marginally lower *FOXM1* expression was observed in the presence of any *EGFR* mutations (Fig. 3), regardless of the mutation. No difference was observed in *FOXM1* expression with *KRAS* nor *TP53* mutated. There was significantly higher *FOXM1* expression when *STK11* was mutated than with no mutations (p < .001).

Comparing *FOXM1* expression and the different *KRAS* mutant subtypes, the G12V mutants had the highest median *FOXM1* expression (2.8; range, 1.0 to 2.1), higher than the levels seen with wild-type *KRAS* (3.5; range, 0.0 to 9.0). G12C mutants had the lowest *FOXM1* expression with a median of 0.16 (range, 0.0 to 10.5).
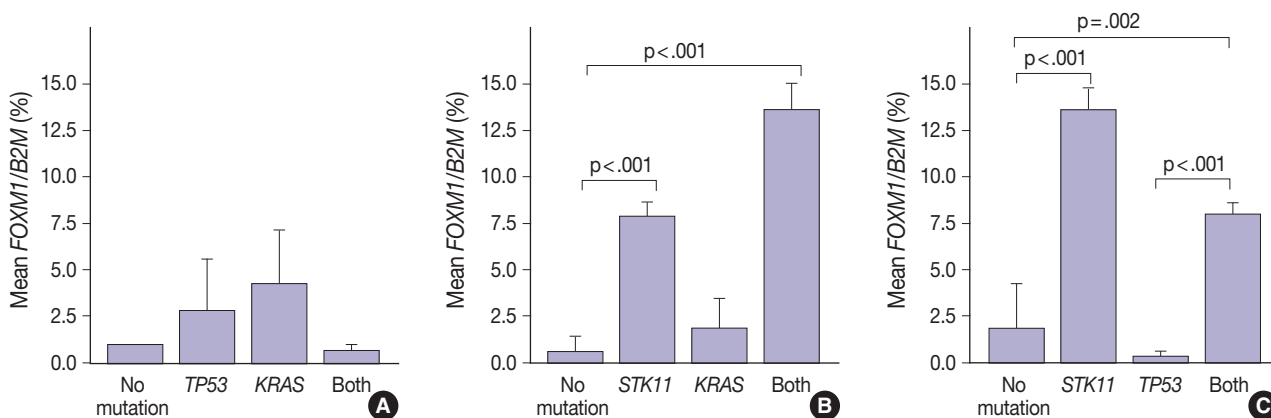
FOXM1 expression patterns in the presence of multiple mutations were dissimilar to patterns seen with SUV for *KRAS* and *TP53* mutations (compare Figs. 2 and 4). Tumors with *KRAS* and *TP53* mutations had increased *FOXM1* expression compared to no mutations or either mutation alone (Fig. 4A). In contrast, the presence of *STK11* with *KRAS* mutations resulted in significantly higher levels of *FOXM1* expression than with no mutation (p < .001) (Fig. 4B). A significant increase was seen in combination with *TP53* versus no mutation and versus *TP53* alone (p = .002 and p < .001, respectively) (Fig. 4C).

Patient outcome studies

To assess predictive value of metabolic state combined with
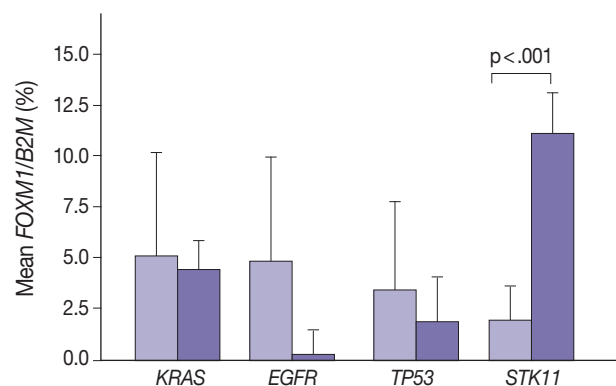
Fig. 3. Tumor *FOXM1* expression in the presence of mutations in *EGFR*, *TP53*, and *STK11* mutations. Cases were classified only on the basis of the indicated mutation.

Fig. 4. *FOXM1* expression patterns in tumors in the presence of multiple mutations. Tumors with *TP53* and *KRAS* mutations alone or together had higher *FOXM1* expression than those with neither mutation (A). Unlike standardized uptake value, tumors with *STK11* mutations showed significantly higher *FOXM1* expression with or without *KRAS* mutations (B) or *TP53* mutations (C).
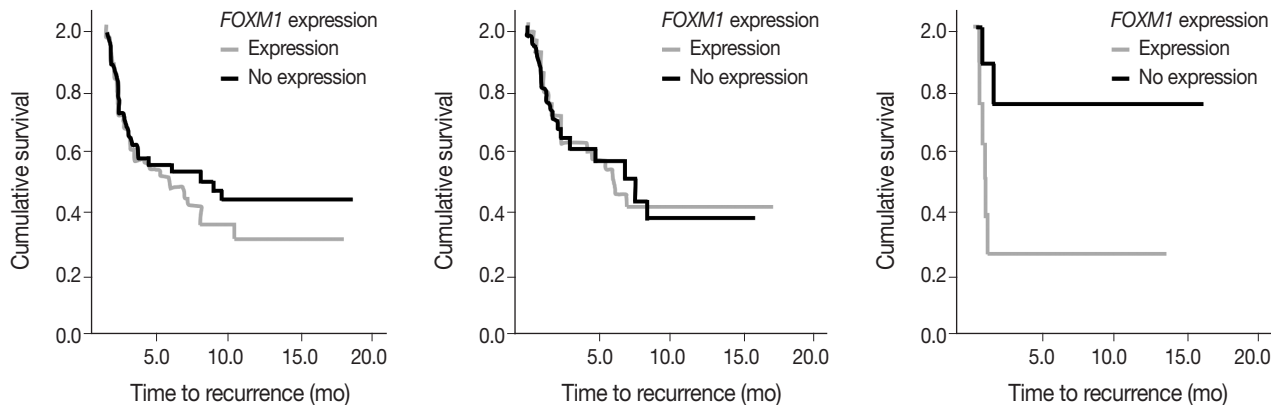
Fig. 5. *FOXM1* expression versus TTR in all cases (n = 104; p = 0.253; left), *KRAS* unmutated cases (n = 67, p = .274, center), and *KRAS* mutated cases (n = 16, p = .033, right).

mutational status, *FOXM1* expression (any expression vs. no expression) in the tumor samples was compared to TTR and OS in early-stage surgically treated patients. There was no significant difference in OS and marginal decrease in TTR when *FOXM1* was expressed versus not expressed. In cases with *KRAS* mutations, however, a significantly shortened TTR was observed when *FOXM1* was expressed (24 months vs. median not reached, respectively; p = .033) (Fig. 5).

DISCUSSION

Identification of somatic variants in tumors is essential in the prognosis and treatment strategy for lung adenocarcinoma. Tumor mutational and glycolytic status can vary in predicting treatment efficacy. The current study examined the relationship between tumor metabolic activity as measured by glucose uptake, gene expression in the glycolysis pathway and mutational status,

with potential consequences on outcome.

Frequencies of the selected mutations in this patient group: *TP53* (42% of cases), *KRAS* (35% of cases), *EGFR* (12% of cases), and *STK11* (10% of cases) reflected reported frequencies of these variants in lung cancer [16]. Co-existing mutations (among the four genes tested) was observed in 10% of cases. In previous studies, the presence of co-existing mutations such as *TP53* and *EGFR* mutations in NSCLC were associated with inferior survival [2]. Others have observed that survival with chemotherapy was longer for patients without *TP53* and *KRAS* mutations compared with patients with *KRAS*, *TP53* mutations, or double mutant tumors [1,17].

Glucose metabolism and the glycolysis pathway are dysregulated in lung cancer. This is a complex issue, with numerous factors involved, including tumor stage, co-morbidities, age, performance status, and tumor mutational state. Metabolic activity may not predict the presence of mutations in cancer genes, such

as *EGFR* [18,19]. Consistent with these reports, no significant relationship between *EGFR* mutation status and SUV was observed in the current study. SUV was increased, however, with co-existing *TP53* and *KRAS* mutations (p = .029) (Fig. 2). *STK11* or any *KRAS* alone were also not related to tumor metabolic status as measured by maximum SUV. Significant differences in SUV in the presence of co-existing mutations were not observed. There was marginally decreased maximum SUV in tumors with co-existing *KRAS + STK11* mutations (p = .141).

In contrast, there was significantly increased glycolytic activity as measured by levels of *FOXM1* expression in the presence of mutated *STK11* (p < .001). Furthermore, tumors with co-existing TP53 or *KRAS + STK11* mutations showed significantly increased *FOXM1* expression (p = .002 and p < .001, respectively). *FOXM1* is downregulated by *TP53* through the *FOXO3* transcription factor to slow DNA repair functions in cells with DNA damage. FoxO3 and FoxM1 transcription factors are also implicated in cancer initiation through metabolic programs [20].

Reported higher levels of *FOXM1* expression in oral cancer tumors with *TP53* mutations than with wild-type *TP53* were not observed here with lung adenocarcinoma [21]. One explanation for this difference is the effect of co-existing mutations, such as *STK11*. *STK11* serine/threonine-protein kinase (also called LKB1) controls the activity of AMPK, to dampen cell metabolism. Human bronchial epithelial cells carrying mutated *KRAS* together with downregulated *STK11* produced squamous cell carcinoma and adenosquamous cell carcinoma when injected into nude mice [15]. Furthermore, Stk11-deficient lung tumors showed primary resistance to treatments that are effective to Kras^{G12D} mutants [16,17]. These results show the potential heterogeneity in outcome of gene inactivation in NSCLC. Differences in PET and *FOXM1* response in *STK11 + KRAS* mutant tumors complicate coordination of tumor progression with metabolic adaptation by gene (*STK11* and *KRAS*) inactivation. FoxM1 protein is activated by Kras which is one of its downstream effectors. *STK11* may also down-regulate Kras activity.

Adding to the complexity are differences in SUV and *FOXM1* expression levels in the presence of the *KRAS* mutant subtypes suggesting that the mutant proteins produced could behave differently within the tumor cells and act through different pathways (causing differences in the progression and/or severity of the disease). The particular point mutation can change the overall stoichiometry of the encoded protein altering the proteins native interactions and normal effects on the cell. These mutation subtypes also interact differently with *FOXM1*, leading to varying levels of expression and activation.

Expression of the *FOXM1* transcription factor gene is highly correlated with the glycolytic pathway. Its expression was observed to be significantly higher in tumor tissue than in non-malignant tissue. PET SUV (also correlated with malignancy) trended lower when *FOXM1* was not expressed than with any *FOXM1* expression. Furthermore, *FOXM1* expression is under epigenetic control, in part, as a target of miR-149. In this study minimum and maximum SUV trended lower when *FOXM1* was not expressed than with any *FOXM1* expression.

FOXM1 expression on its own did not have a significant effect on patient survival (p = .875) nor tumor recurrence (p = .274), but did have a significant negative effect on TTR in patients who also expressed mutant *KRAS*. The effect of *FOXM1* expression on tumor recurrence in cases with *KRAS* mutations (Fig. 5), suggests that *FOXM1* expression may have a minor effect on the tumor phenotype, but could still be a viable prognostic factor, especially in the presence of other cancer gene mutations [22]. The phosphatidylinositol 3-kinase pathway signals growth and survival and helps drive the glycolytic phenotype of cancer cells by increasing cellular glucose uptake and glycolysis [23]. HNSCC patients with high levels of *FOXM1* expression in the presence of *TP53* mutations have been observed to have poor survival outcomes [21]. The presence of *FOXM1* expression could indicate a higher chance of tumor recurrence, which can then be used by a provider when deciding on the intensity of the course of treatment [24,25].

These observations are limited to the four genes investigated in this study. The effects of co-existing mutations suggest that cancer cells with high tumor mutational burden (coding somatic mutations/Mb of tumor DNA) may have further differences in metabolic characteristics. Tumor mutational burden also affects immune characteristics of tumors which contribute to recurrence and survival following treatment. Further studies with more comprehensive mutational analysis would address this question.

With the effects of mutation state on *FOXM1* expression, further studies on outcome were performed comparing *FOXM1* expression and outcome. *STK11* mutations were significantly related to increased *FOXM1* expression; however, numbers were not sufficient for analysis. Although measurement of *FOXM1* gene expression is not currently a practical method for tumor assessment, its comparison to PET activity shows a degree of complexity in metabolic activity in tumor cells with and without mutations. The effect of *KRAS* mutations on outcome with and without *FOXM1* expression suggests that both metabolic and mutational status affect tumor characteristics, and predicted patient outcome.

ORCID

Waqas Mahmud: https://orcid.org/0000-0002-2773-1749
Lela Buckingham: https://orcid.org/0000-0002-2735-0946

Author Contributions

Conceptualization: AG, LB, WM.
Data curation: AG, LB, WM.
Formal analysis: AG, LB, WM.
Funding acquisition: LB.
Investigation: AG, LB, WM.
Methodology: AG, LB, WM.
Project administration: LB.
Resources: LB, WM.
Software: AG, LB, WM.
Supervision: LB.
Validation: WM.
Visualization: AG, LB, WM.
Writing—original draft: AG.
Writing—review & editing: WM, LB.

Conflicts of Interest

The authors declare that they have no potential conflicts of interest.

REFERENCES

1. Tomasini P, Mascaux C, Jao K, et al. Effect of coexisting *KRAS* and *TP53* mutations in patients treated with chemotherapy for non-small-cell lung cancer. Clin Lung Cancer 2019; 20: e338-45.

2. Aggarwal C, Davis CW, Mick R, et al. Influence of *TP53* mutation on survival in patients with advanced *EGFR*-mutant non-small-cell lung cancer. JCO Precis Oncol 2018 Aug 31 [Epub]. https://doi.org/10.1200/PO.18.00107.

3. Ding M, Li F, Wang B, Chi G, Liu H. A comprehensive analysis of WGCNA and serum metabolomics manifests the lung cancer-associated disordered glucose metabolism. J Cell Biochem 2019; 120: 10855-63.

4. Cairns RA, Harris IS, Mak TW. Regulation of cancer cell metabolism. Nat Rev Cancer 2011; 11: 85-95.

5. Soga T. Cancer metabolism: key players in metabolic reprogramming. Cancer Sci 2013; 104: 275-81.

6. Park HL, Yoo IR, Boo SH, et al. Does FDG PET/CT have a role in determining adjuvant chemotherapy in surgical margin-negative stage IA non-small cell lung cancer patients? J Cancer Res Clin Oncol 2019; 145: 1021-6.

7. Brun C, Gay P, Cottier M, et al. Comparison of cytology, chest computed and positron emission tomography findings in malignant pleural effusion from lung cancer. J Thorac Dis 2018; 10: 6903-11.

8. Vander Heiden MG, Cantley LC, Thompson CB. Understanding the Warburg effect: the metabolic requirements of cell proliferation. Science 2009; 324: 1029-33.

9. Cui J, Shi M, Xie D, et al. *FOXM1* promotes the warburg effect and pancreatic cancer progression via transactivation of LDHA expression. Clin Cancer Res 2014; 20: 2595-606.

10. Liao GB, Li XZ, Zeng S, et al. Regulation of the master regulator FOXM1 in cancer. Cell Commun Signal 2018; 16: 57.

11. He Y, Yu D, Zhu L, Zhong S, Zhao J, Tang J. miR-149 in human cancer: a systemic review. J Cancer 2018; 9: 375-88.

12. Xu K, Liu X, Mao X, et al. MicroRNA-149 suppresses colorectal cancer cell migration and invasion by directly targeting forkhead box transcription factor FOXM1. Cell Physiol Biochem 2015; 35: 499-515.

13. Wierstra I, Alves J. FOXM1, a typical proliferation-associated transcription factor. Biol Chem 2007; 388: 1257-74.

14. Wang IC, Ustiyan V, Zhang Y, Cai Y, Kalin TV, Kalinichenko VV. Foxm1 transcription factor is required for the initiation of lung tumorigenesis by oncogenic Kras(G12D.). Oncogene 2014; 33: 5391-6.

15. Wang IC, Snyder J, Zhang Y, et al. Foxm1 mediates cross talk between Kras/mitogen-activated protein kinase and canonical Wnt pathways during development of respiratory epithelium. Mol Cell Biol 2012; 32: 3838-50.

16. Catalogue of Somatic Mutations in Cancer (COSMIC) [Internet]. Hinxton: Wellcome Sanger Institute; 2020 [cited 2020 Feb 2]. Available from: https://cancer.sanger.ac.uk/cosmic.

17. Arbour KC, Jordan E, Kim HR, et al. Effects of co-occurring genomic alterations on outcomes in patients with *KRAS*-mutant non-small cell lung cancer. Clin Cancer Res 2018; 24: 334-40.

18. Zhu L, Yin G, Chen W, et al. Correlation between *EGFR* mutation status and F(18) -fluorodeoxyglucose positron emission tomography-computed tomography image features in lung adenocarcinoma. Thorac Cancer 2019; 10: 659-64.

19. Kim HS, Mendiratta S, Kim J, et al. Systematic identification of molecular subtype-selective vulnerabilities in non-small-cell lung cancer. Cell 2013; 155: 552-66.

20. Saavedra-Garcia P, Nichols K, Mahmud Z, Fan LY, Lam EW. Unravelling the role of fatty acid metabolism in cancer through the FOXO3-FOXM1 axis. Mol Cell Endocrinol 2018; 462: 82-92.

21. Tanaka N, Zhao M, Tang L, et al. Gain-of-function mutant p53 promotes the oncogenic potential of head and neck squamous cell carcinoma cells by targeting the transcription factors FOXO3a and FOXM1. Oncogene 2018; 37: 1279-92.

22. Shimamura T, Chen Z, Soucheray M, et al. Efficacy of BET bromodomain inhibition in Kras-mutant non-small cell lung cancer. Clin Cancer Res 2013; 19: 6183-92.

23. Kompier LC, Lurkin I, van der Aa MN, van Rhijn BW, van der Kwast TH, Zwarthoff EC. *FGFR3*, *HRAS*, *KRAS*, *NRAS* and *PIK-3CA* mutations in bladder cancer and their potential as biomarkers for surveillance and therapy. PLoS One 2010; 5: e13821.

24. He SY, Shen HW, Xu L, et al. *FOXM1* promotes tumor cell invasion and correlates with poor prognosis in early-stage cervical cancer. Gynecol Oncol 2012; 127: 601-10.

25. Wang IC, Meliton L, Ren X, et al. Deletion of Forkhead Box M1 transcription factor from respiratory epithelial cells inhibits pulmonary tumorigenesis. PLoS One 2009; 4: e6609.